Original Research Article

Optoelectronic Performances of Au and CuO Nanoparticles Incorporated P3HT/PCBM Based Organic Photovoltaic Devices

ABSTRACT

Direct conversion of sun energy to electrical energy using nanostructured organic/inorganic hybrid semiconductors is one of the best solutions for today's energy crisis. In particular, researchers are turning their attention to incorporation of metal or transition metal oxide nanoparticles (NPs) into the active layer of polymer solar cells (PSCs). The design approaches for incorporation of metal NPs is based on localized plasmonic resonance effect (LSPR) which can be used to enhance the optical absorption in photovoltaic devices. Meanwhile, the transition metal oxide NPs such as Cuprous oxide (CuO) NPs in the active layer play a key role as light harvesting centers, charge particle hopping centers and surface morphology developers enabling a considerable reduction in the physical thickness of photovoltaic absorber layers. In this study, to enhance the power conversion efficiency (PCE) of the polymer solar cells (PSCs), Au NPs and CuO NPs are incorporated into P3HT/PCBM active layer. Addition of Au and CuO NPs increased the power conversion efficiency by up to 48.7% compared to a reference cell without Au or CuO-NPs. The short circuit current(Jsc) of the cells containing 0.05 mg of Au and CuO NPs was measured at 7.218 mA/cm^2 compared to 5.338 mA/cm^2 in the reference cells without nanoparticles; meanwhile, the external quantum efficiency(EQE) increased from 45% to 68.5%, showing an enhancement of 52.2%. Au and CuO-NPs improved the charge collection at the anode, which results in higher short circuit current and fill factor.

Keywords: Plasmonic effect; Polymer Solar Cells; Au NPs; CuO NPs; P3HT

1. INTRODUCTION

Bulk heterojunction (BHJ) polymer solar cells (PSCs) which are based on conjugated polymer donor and fullerene derivative acceptor materials have attracted much attention due to the efficient charge transfer from conjugated polymers to fullerene derivatives. Compared to inorganic solar cells, Polymer solar cells (PSCs) usually have one important hindrance for the efficiency improvement with insufficient light absorption due to the thin active layer which is restricted by the short exciton diffusion length and low carrier mobility. Efficient sun energy harvesting requires the compounds to absorb strongly in the visible region of the spectrum [1-3].

Illuminated metallic nanoparticles (NPs) such as Au and other metallic nanostructures can be used to enhance the light absorption of the polymer thin films due to the localized surface plasmon resonance (LSPR) effect which enables to a remarkable enhancement of local electromagnetic fields [4,5]. The LSPR of metallic NPs is referred to as the collective oscillation of electrons residing on the metallic NPs are excited by the incident light photons

at the resonant frequency [6]. The LSPR excitation of the metallic NPs results in improved electromagnetic fields, light absorption and scattering due to their physical and elemental parameters, which leads to enhanced device performances. Considering the strong LSPR effect of the metallic NPs such as Ag and Au, many researchers have widely investigated them for different technological applications including photovoltaic device fabrications [7,8]. Brown et al [9] have shown that the metallic nanostructures in the active layer can scatter the incident photons through a long propagation path resulting in a higher light absorption and photocurrent generation of PSCs. Lu et al [10] reported 20% enhancement of power conversion efficiency of Au and Ag incorporated PSCs due to the LSPR effect.

On the other hand, NPs of transition metal oxides such as copper oxide nanoparticles (CuO NPs) have gained special attention due to the low cost, non-toxic, and high optical absorption capabilities. CuO is a p-type semiconductor with a direct band gap energy of 1.5 eV which is close to the ideal energy gap of 1.4 eV for fabricating the high optical absorbing solar cells [11–14]. In the previously reported work by the author [15-17] has shown that incorporation of the CuO NPs in the active layer increased the power conversion efficiency (PCE) of the solar cells by 40.6%. However, there is no reported work for incorporating both Au NPs and CuO NPs in the same active layer of PSCs. Therefore, this study will be the first effort that extends to investigate the effect of the CuO NPs together with Au NPs in the active layer.

This study will be focused on the impact of the incorporation both Au and CuO NPs into the P3HT/PCBM (poly (3-hexylthiophene)/ [6, 6]-phenyl-C70-butyric acid methyl ester) active layer of the polymer solar cell devices. The short-circuit current (JSC) and fill factor (FF) are improved with an appropriate amount of Au and CuO NPs incorporated in the active layer. The optoelectronic parameters are comparatively studied by UV absorption, SEM, EQE, AFM and solar simulation. Therefore, this work will be contributed to better understanding the uses of Au NPs and CuO NPs combination in the active layer for enhancing PSCs performances.

2. EXPERIMENTAL METHODS

2.1 Materials

Poly(3-hexylthiophene) (P3HT) (Rieke Metals), phenyl-C70butyric acid methyl ester (PC70BM) (SES Research), Nanoparticles of gold (Au) (15 nm diameter) and Nanoparticles of CuO (10-30 nm diameter) (nanocs.com), Glass substrates measuring 24 x 80 x 1.2 mm (12 Ω/cm^2) with an Indium Tin Oxide (ITO) conductive layer of 25-100 nm (nanocs.com) and Aluminium coils with a diameter of 0.15 mm (Ted-Pella, Inc.) were used as received. poly(3,4ethylenedioxythiophene)-poly(styrenesulfonate) (PEDOT/PSS) mixed in distilled water was obtained from Sigma Aldrich and it was mixed with an equal amount of distilled water. All processing and characterization work of the PSC devices were conducted under the same experimental conditions.

2.2 Device Fabrication

The conductive glass substrates were ultrasonically cleaned with ammonium hydroxide, hydrogen peroxide, distilled water, methyl alcohol, and isopropyl alcohol; successively. The fabrication of polymer based solar cells containing Au-NPs was carried out in a N_2 filled glove box. The P3HT-PC70BM blend was obtained by diluting equal amounts of regioregular P3HT and PC70BM (10 mg each) with 2 ml of chlorobenzene (C6H5Cl) and mixing for 14 hours at 50^oC. The 0.05 mg of Au-NPs (15 nm diameter) and 0.6 mg of CuO-NPs (10-30 nm

diameter) were added to the mixture, so that the weight ratio of P3HT/PCBM/Au-NPs/CuO-NPs in the final blends was 10:10:0.05:0.6.

The solar cell devices were spun coated in a glove box with N_2 atmosphere. A 40 nm-thick PEDOT/PSS layer, which serves as a thin hole-transport layer, was spun coated at a rotational velocity of 4000 rpm, followed by heating at 120°C for 20 minutes in air. When the temperature of the samples reached the ambient temperature, the blends with P3HT:PC70BM:Au-NPs:CuO NPs solution was spun coated for two minutes at 1000 rpm. The active layers measured 120 nm in average thickness and 0.12 cm^2 in surface area. A schematic illustration of the layered structure of the fabricated devices is shown in Figure 1.

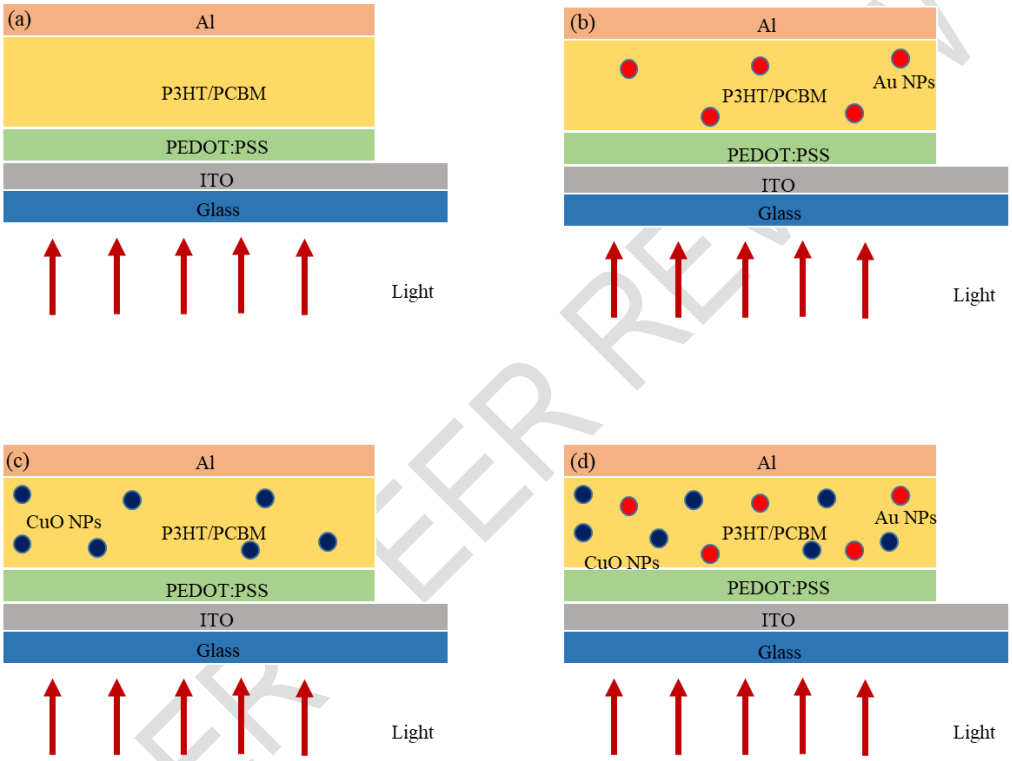

Fig. 1. Schematic illustration of polymer solar cells: (a) Reference solar cell without nanoparticles, (b) Au NPs incorporated solar cells, (c) CuO NPs incorporated cells, (d) Au and CuO NPs incorporated solar cells.

2.3 Characterization

Current density–voltage (J-V) characterization was carried out for all PSCs using a UV solar simulator with an AM 1.5G filter and a lamp intensity of 100 mW/cm^2. A source meter (Keithley 2400) was used to obtain the J-V measurements. Device parameters; such as short circuit current (Jsc), open circuit voltage (Voc), fill factor (FF) and power conversion efficiency (PCE) were recorded under ambient conditions. A quantum efficiency measurement kit (Newport-425) embedded in the solar cell simulator was used to obtain EQE values. A PerkinElmer LAMBDA 650 spectrophotometer was used to obtain the optical properties of cells.

An Agilent 5420 atomic force microscope(AFM) was used to analyze the surface morphology. The Pico Image Basics and Gwyddion software were utilized to determine the root mean square roughness (σrms) of surface under ACAFM noncontact mode with set point 1.60, I-gain of 10 and scanned area of 2x2 μm. The layer structures of the fabricated solar cells were analyzed using a scanning electron microscope with an energy dispersive x-ray detector (FEG-SEM Hitachi S-4800).

3. RESULTS AND DISCUSSION

The power conversion efficiency of the devices with four different concentrations of Au and CuO NPs were fabricated and tested under simulated 100 mW cm^{-2} AM1.5G illumination. The table 1 indicates the photovoltaic parameters, such as Jsc, Voc, fill factor (FF) of all the fabricated devices.

Table 1. Performance parameters of hybrid solar cells

CuO NPs (mg)	Au NPs (mg)	J_{sc} (mA/cm^2)	V_{oc} (V)	FF (%)	PCE (%)
0	0.00	5.338	0.65	61	2.114
0	0.05	6.228	0.65	66	2.672
0.6	0.00	6.829	0.66	66	2.975
0.6	0.05	7.218	0.66	66	3.144

Summarized data demonstrates that the Voc remained nearly the same for all the four types of devices of no NPs, 0 mg CuO NPs + 0.05 mg Au NPs, 0.6 mg CuO NPs + 0 mg Au NPs, and 0.6mg CuO NPs + 0.05 mg Au NPs in the P3HT/PCBM active layers. To match the energy levels of the commonly used electron acceptor PCBM with the energy levels of P3HT donor, it is a very crucial factor to tune both the highest occupied molecular orbital (HOMO) and the lowest unoccupied molecular orbital (LUMO) of the organic materials. The Voc is directly related to the energy difference between the LUMOs of donor and acceptor materials which should be larger than 0.3 eV for efficient excitonic dissociation [18, 19]. But, the Voc of organic solar cells is restricted by the difference between the HOMO of the donor and the LUMO of the acceptor. However, above results imply that the positions of the HOMO of the donor and the LUMO of the acceptor were not altered by Au or CuO NPs in the active layer. It is clear that the Jsc increased from 5.338 mA/cm^2 to 6.228 mA/cm^2 by adding Au NPs in the active layer. Furthermore, the Jsc was increased to 6.829 mA/cm^2 after adding CuO NPs into the P3HT/PCBM active layer. The highest Jsc was exhibited by the PSCs which contained both Au and CuO NPs in the active layer. The FF values were enhanced from 61% to 66%. However, the FF value remained unchanged at 66% without depending on the types of the NPs. The FF explains the combination of the series resistance (Rs) and shunt resistance (Rsh) of the device. Rs represents the sum of contact resistance on the front/back surfaces and the ohmic resistances. Shunt resistance is mainly due to the imperfections on the device surface [20]. The Au NPs and CuO NPs did not show a significant influence on the resistance of the device. These improved Jsc and FF influenced on PCE and it was enhanced from 2.114% to 3.144% by incorporating Au and CuO NPs in the same P3HT/PCBM active layer. In spite of this behavior of Voc, the increase in PCE translates to a 48.7% total enhancement in the P3HT/PCBM active layer containing 0.05 mg of Au NPs and0.6 mg of CuO NPs in comparison to the reference cells. Figure 2 shows J-V characteristics curves of ITO/PEDOT: PSS/ P3HT /PCBM/Al solar cells with Au NPs and

CuO NPs in the P3HT/PCBM active layer and J–V characteristic of pristine device without Au or CuO NPs as the reference devices.

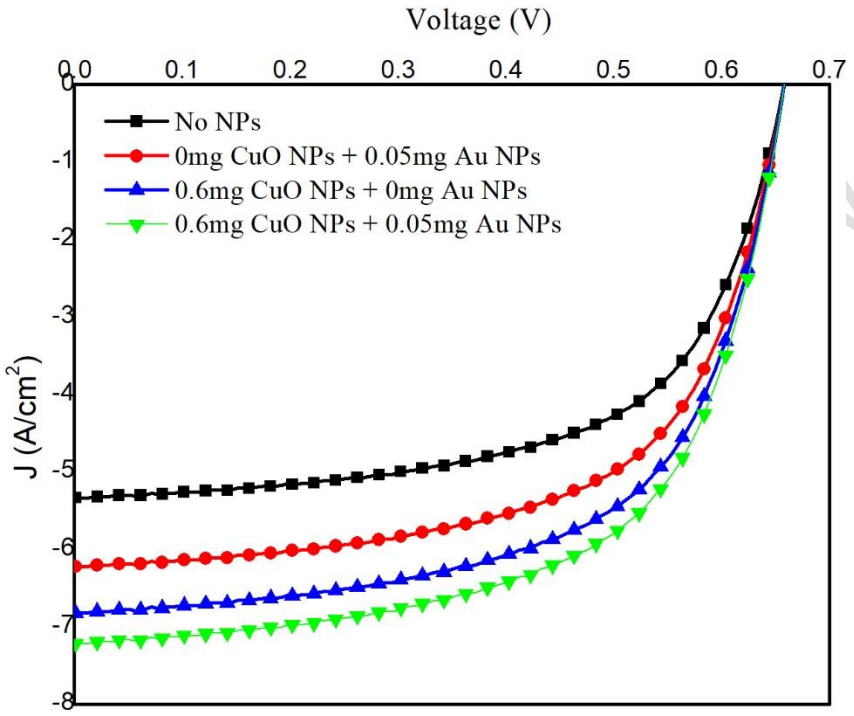

Fig. 2. J-V characteristics of P3HT/PCBM/Au/CuO NPs polymer solar cells

The Jsc of the solar cell device has a linear relationship with the EQE which is theoretically indicated as equation 1.

$$J_{sc} = \frac{q}{\hbar C}\int_{\lambda_{min}}^{\lambda_{max}} EQE\ P_{in}(\lambda)\ \lambda\ d\lambda \qquad (1)$$

where q is the value of the charge, $\hbar$ is the reduced Planck constant, C and λ are the velocity and the wavelength of the light respectively.

The EQE is a ratio between the incident photons on the solar cell from the input light and the generated free charge carriers by the solar cell. The EQE can be modified as internal quantum efficiency (IQE) neglecting reflectance and transmittance of the incident photons to consider only the portion of the absorbed light by the active region. In the organic semiconductor based solar cells, EQE can be determined by five major factors which are composed with inherent efficiency components [17] which can be shown in equation 2.

$$EQE = \eta_A . \eta_{diff} . \eta_{diss} . \eta_{tr} . \eta_{cc} \qquad (2)$$

Here, η_A, η_{diff}, η_{diss}, η_{tr} and η_{cc} are represented the light absorption efficiency, the excitonic diffusion efficiency, the excitonic dissociation efficiency, the charge transport efficiency, and the electrons-holes collection efficiency respectively.

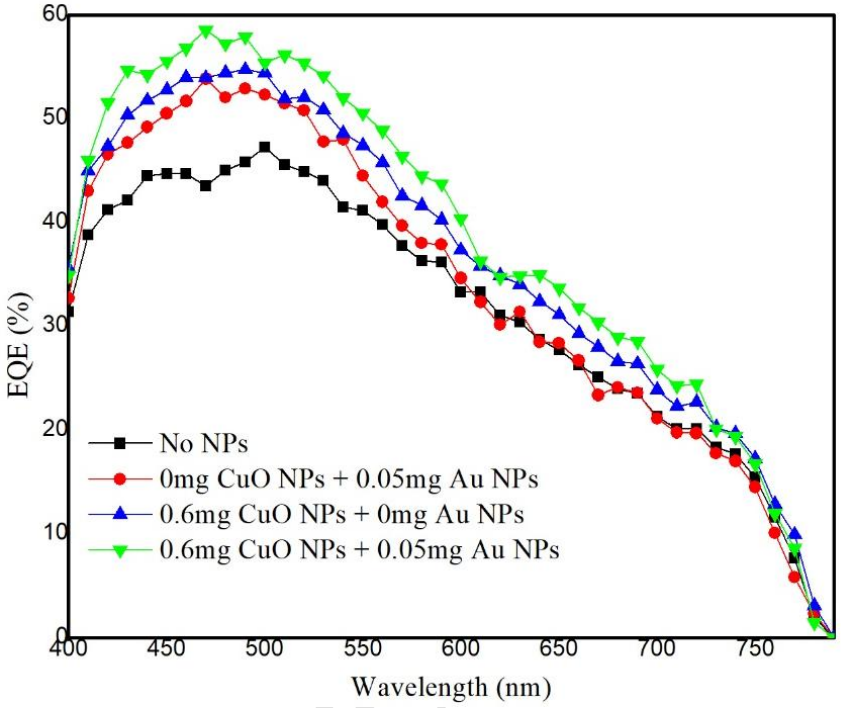

Fig. 3. EQE of the hybrid solar cells with various concentrations of Au and CuO NPs in the P3HT/PCBM active layer

The shape of the EQE can be used to understand the material properties of the device and it is strongly correlated to the junction thickness and blend composition of the active layer. Furthermore, the shape of the EQE explains the mechanisms for free carrier generation in the active layer region. To confirm the accuracy of the J-V measurements, the EQE spectrum of the devices which were fabricated using four different concentrations of Au and CuO NPs was measured. The EQE curves are shown in Figure 3. Corresponding EQE spectra for solar cells are improved from 45% to 68.5%. These all devices exhibit efficient photoconversion in the range of 400–750 nm, with EQE peak values from 45% to 68.5%. To obtain such higher EQE values, it is requisite to accomplish enhanced and efficient light absorption, exciton diffusion, charge carrier separation and charge collection at the electrodes. Therefore, this improved EQE conduct to better elucidate improved Jsc relevant to the enhanced free carrier generation.

The metal nanostructures have one of the most important properties is plasmonic behavior which is the collective oscillation of free electrons in the metal structure. Other properties such as reflection and transmission occur when the frequency of the incident light is below the plasma frequency and above the plasma frequency respectively. Frequently, the range of the plasma frequency of metals is in the ultraviolet domain, which leads plasma reflective

in the visible range. The plasmonic energy of such structures can be written as equations 3 and 4.

$$E_0 = \hbar\omega_0 \quad (3)$$

$$\omega_0 = \hbar\sqrt{\frac{ne^2}{m\varepsilon_0}} \quad (4)$$

where *n* is the electron density, *e* is the electron charge, *m* is the electron mass, ε_0 is the permittivity of the free space, $\hbar$ is the Planck constant, and ω_0 is the plasmon frequency.

On the other hand, surface plasmons related to a metallic nanoparticle can be considered as localized surface plasmons (LSPs). When the light shine on the metallic nanoparticles, the electrons associated with the surface of the NPs are subjected to collective oscillate called LSPs as shown in figure 4. In addition, the Mie solution to Maxwell's equations for the spherical nanoparticles explains the scattering and absorption phenomena of incident light. The correlation of the absorption cross-section (σ_{ab}) and the scattering cross-section (σ_{sc}) of the metal nanoparticles to the extinction cross-section (σ_{ext}) can be shown in equation 5 [21, 22].

$$\sigma_{ext} = \sigma_{ab} + \sigma_{sc} \quad (5)$$

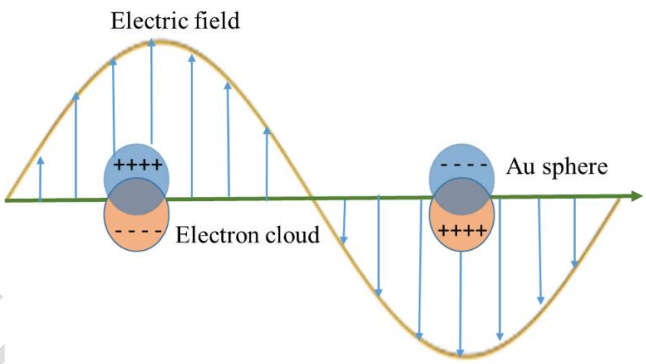

Fig. 4. localized surface plasmon resonance (LSPR), resulting from the collective oscillations of delocalized electrons in response to an external electric field.

Photo absorption and carrier generating ability of a polymer thin film are represented by the photon absorption (η_A) efficiency. The light absorption of a semiconductor thin film is controlled by the energy band structure, absorption coefficient and the thickness of the photoactive layer. However, Au NPs improve the light absorption of the thin films due to the localized surface plasmon resonance (LSPR) which contributes to the significant enhancement of local electromagnetic fields and thus improves the optical properties of the nanostructured devices [23, 24].

The CuO NPs can be considered as the P3HT tuning materials due to its suitable energy band structure and photo-electrons donor properties. Therefore, CuO NPs may increase the exciton generation and dissociation process in the PSCs. Also, CuO NPs play a role being charge hopping centers for charge carriers enabling high charge mobility within the structure. N.R. Dhineshbabu *et al* [12] have reported that CuO NPs has shown high absorbance at UV region, and then it decreases exponentially in the visible region near IR region. So the CuO NPs are very low absorptive at the visible region and is more convenient for the solar cells.

Also, the CuO thin film has high optical absorption coefficient ($\alpha \geq 10^4 cm^{-1}$) which is conducive to increasing the probability of direct transitions occurrence. On the other hand, the CuO nanoparticles consists of small nanocrystalline clusters with different orientation of the single crystal diffraction pattern and, the CuO nanoparticles encourage the formation of P3HT crystallites in the structure reducing the charge carrier diffusion length. Therefore, these CuO NPs clusters and crystallized P3HT enhance the charge carrier hopping process minimizing the charge recombination. The UV-vis absorption measurements of the solar cells with and without Au/CuO-NPs in the active layer are shown in Figure 5.

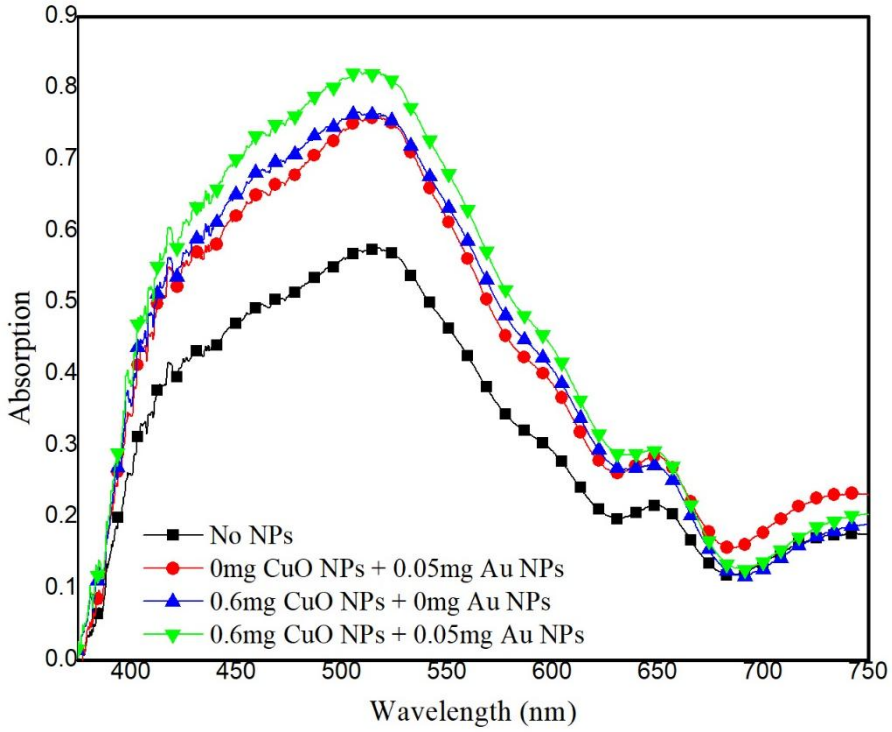

Fig. 5. Optical absorption spectra of the hybrid solar cells

The absorption spectrum of the P3HT/PCBM/Au/CuO-NPs device shows a significant improvement after incorporating the both Au and CuO NPs in the P3HT/PCBM active layer. The UV-vis absorption, EQE and J_{sc} measurements were significantly increased showing same trend. Therefore, it can be identified that the plasmonic effect (LSPR) of Au NPs and absorption properties of CuO NPs play significant role in enhanced PCE of the solar cell devices.

The AFM images of the P3HT/PCBM with different concentrations of Au and CuO NPs dispersed films were obtained to understand the surface morphology of the active layer as shown in figure 6. Significantly different morphologies were observed for these four types of devices in their AFM images. The root-mean-square roughness (R_{rms}) is linearly correlated with the interfacial surface area between the active layer and PEDOT: PSS hole collection layer or Al cathode. The increase of the interfacial surface area leads to the efficient dissociation of excitons into holes and electrons. The P3HT/PCBM layer showed a relatively smooth surface with root-mean-square roughness (R_{rms}) value of 0.10 nm. It was noticed that the R_{rms} value of the P3HT/PCBM layer was increased with increasing the concentration of the NPs in the P3HT/PCBM blend. The R_{rms} of the device with 0.05 Au NPs was 0.81 nm.

However, it was exhibited 0.32 nm in the samples containing 0.6 mg of CuO NPs. Furthermore, the R_{rms} value was enhanced up to 0.91 nm of the P3HT/PCBM layers incorporated with both CuO and Au NPs as shown in table 2.

Table 2: R_{rms} values of the PSCs with different concentration of Au/CuO NPs

Sample	CuO NPs (mg)	Au NPs (mg)	R_{rms} (nm)
(a)	0.00	0.00	0.10
(b)	0.00	0.05	0.81
(c)	0.60	0.00	0.32
(d)	0.60	0.05	0.91

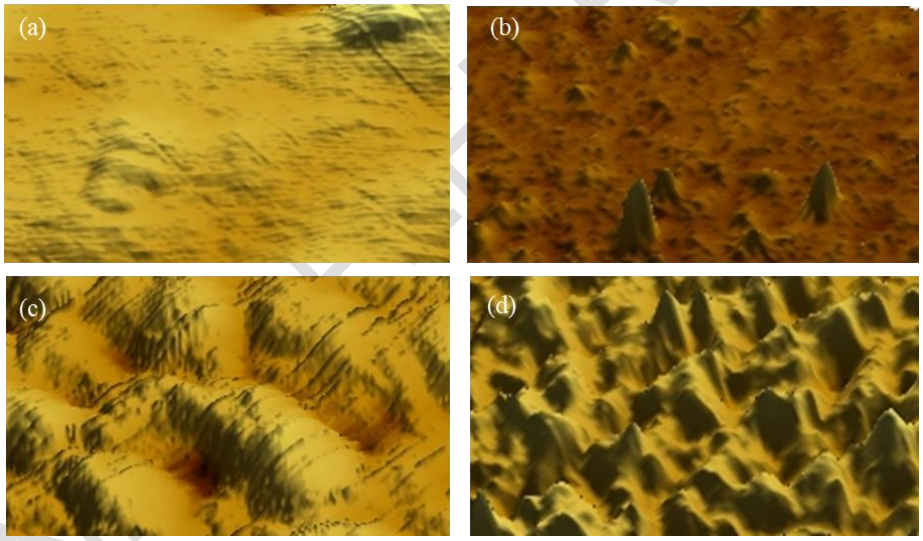

Fig. 6. AFM images for P3HT/PCBM layers with (a) no NPs, (b) 0 mg CuO NPs + 0.05 mg Au NPs,(c) 0.6 mg CuO NPs + 0 mg Au NPs, (d) 0.6 mg CuO NPs + 0.05 mg Au NPs

On the other hand, this increased surface roughness contributes to enlarge the interfacial contact area between the PEDOT: PSS and P3HT/PCBM-CuO/Au NPs layers, allowing high efficient hole collection at the anode and hence improve the J_{sc} and shape of the FF. Also, this increased surface roughness of the cells with Au and CuO NPs, which is an evidence of adequate space for P3HT crystallites to form in the active layer structure. Higher P3HT crystals discourage the fully amorphous PCBM molecules to dissolved in the P3HT domain, thus promoting the aggregation of PCBM, which will contribute to PCBM/P3HT phase separation. The SEM images of the hybrid structure of the fabricated PEDOT: PSS/ P3HT: PCBM/Au-CuO NPs/device are shown in Figure 7. The Au and CuO-NPs added the

P3HT/PCBM active layer was approximately in the range of 100-160 nm thickness. It is helpful to eliminate the charge recombination losses in the devices. The thickness of the PEDOT: PSS hole transport layer was estimated as 40 nm.

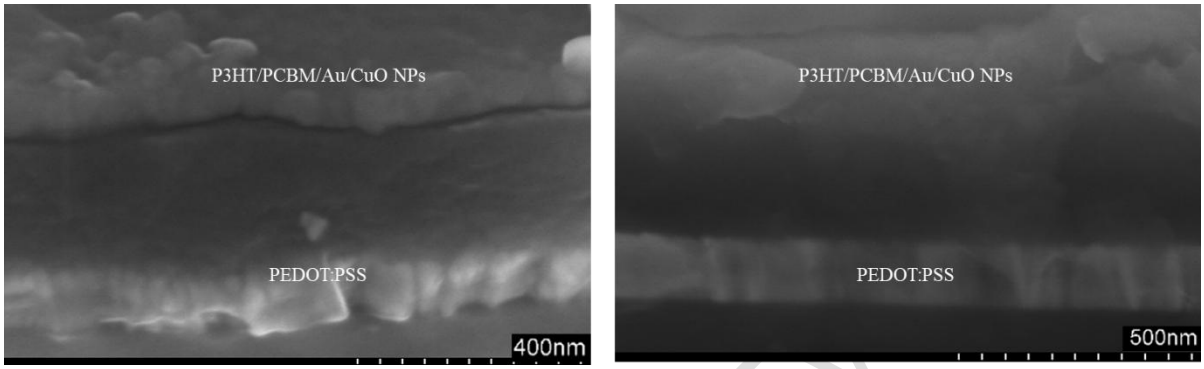

Fig. 7. SEM images of the P3HT/PCBM/Au/CuO NPs hybrid polymer solar cell

4. CONCLUSION

In this study, Au and CuO-NPs were added to the P3HT/PCBM layer of solar cells in order to increase the power conversion efficiency. The PCE increased from 2.114 to 3.144% in the cells containing 0.05 mg Au-NPs and 0.6mg CuO-NPs, which is equivalent to 48.7% improvement in efficiency. The higher performance is attributed to enhanced UV-vis absorption, EQE and Jsc. The optical absorption spectrum changed significantly after the presence of Au-NPs in the P3HT/PCBM active layer due to the strong near field around Au-NPs. EQE of the solar cells increased due to increased hole and electron polaron mobilities in cells with Au and CuO NPs. AFM analysis showed an increase in surface roughness of the P3HT/PCBM active layer with Au and CuO NPs, which is an indication of larger space for P3HT crystallites to form. Also, the FF was enhanced with adding these Au and CuO NPs in the cells.

CONSENT (WHERE EVER APPLICABLE)

"All authors declare that 'written informed consent was obtained from the patient (or other approved parties) for publication of this case report and accompanying images. A copy of the written consent is available for review by the Editorial office/Chief Editor/Editorial Board members of this journal."

ETHICAL APPROVAL (WHERE EVER APPLICABLE)

"All authors hereby declare that all experiments have been examined and approved by the appropriate ethics committee and have therefore been performed in accordance with the ethical standards laid down in the 1964 Declaration of Helsinki."

COMPETING INTERESTS DISCLAIMER:

Authors have declared that no competing interests exist. The products used for this research are commonly and predominantly use products in our area of research and country. There is absolutely no conflict of interest between the authors and producers of the products because we do not intend to use these products as an avenue for any litigation but for the advancement of knowledge. Also, the research was not funded by the producing company rather it was funded by personal efforts of the authors.

REFERENCES

1. Dang MT, Hirsch L, and Wantz G. P3HT: PCBM, Best Seller in Polymer Photovoltaic Research. Adv. Mater. 2011; 23 (31): 3597-3602.
2. Wanninayake A, Church B, Abu-Zahra N. Effect of ZnO Nanoparticles on the Power Conversion Efficiency of Organic Photovoltaic Devices Synthesized with CuO Nanoparticles, AIMS Mater. Sci. 2016; 3(3): 927-937.
3. Li G, Shrotriya V, Yao Y, and Yanga Y. Investigation of annealing effects and film thickness dependence of polymer solar cells based on poly(3-hexylthiophene). J. Appl. Phys.2005; 98: 043704.
4. Sepúlveda B, Angelomé PC, Lechuga LM, Liz-Marzán LM. LSPR-based nanobiosensors. nano today. 2009;4(3): 244–251.
5. Bansal A, Sekhon JS, Verma SS. Scattering efficiency and LSPR tunability of bimetallic Ag, Au, and Cu nanoparticles. Plasmonics,2014; 9(1): 143–150.
6. Liu D, Li L, You T. Superior catalytic performances of platinum nanoparticles loaded nitrogen-doped graphene toward methanol oxidation and hydrogen evolution reaction. J. Colloid Interface Sci. 2017; 487: 330–335.
7. Fu L, Li C, LY, Chen S, Long Y, Zeng R. Simultaneous determination of iodide and bromide using a novel LSPR fluorescent Ag nanocluster probe. Sens. Actuators B Chem. 2017; 240: 315–321.
8. Reisdorffer F, Haas O, Le Rendu P, and Nguyen TP. Cosolvent effects on the morphology of P3HT: PCBM thin films. Synthetic Met. 2012; 161: 2544–8.
9. Brown MD, Suteewong T, Kumar RSS, D'Innocenzo V, Petrozza A, Lee MM, Wiesner U, Snaith HJ. Plasmonic dye-sensitized solar cells using core-shell metal-insulator nanoparticles. Nano Letters.2011:11:438-445
10. Lu L, Luo Z, Xu T, and Yu L. Cooperative Plasmonic Effect of Ag and Au Nanoparticles on Enhancing Performance of Polymer Solar Cells. Nano Lett. 2013; 13(1): 59-64.
11. Sun, B, Marx E, and Greenham NC. (2003) Photovoltaic devices using blends of branched CdSe nanoparticles and conjugated polymers. Nano Lett. 2003; 3: 961–3.
12. Dhineshbabu NR, Rajendran V, Nithyavathy N, Vetumperumal R. Study of structural and optical properties of cupric oxide nanoparticles. ApplNanosci.2016; 6:933–939
13. Sun Y, Liu T, Kan Y, Gao K, Tang B, Li Y. Flexible organic solar cells: Progress and challenges. Small Sci. 2021; 1: 2100001.
14. Qin J, Lan, Chen S, Huang F, Shi H, Chen W, Xia H, Sun K, Yang C. Recent progress in flexible and stretchable organic solar cells. Adv. Funct. Mater. 2020; 5: 2002529.

15. Finn M, Martens C. J, Zaretski A. V, Roth B, Søndergaard R. R, Krebs F. C, Lipomi D. J. Mechanical stability of roll-to-roll printed solar cells under cyclic bending and torsion. Sol. Energy Mater. Sol. Cells 2018; 174: 7-15.
16. Meng L, Zhang Y, Wan X, Li C, Zhang X, Wang Y, Ke X, Xiao Z, Ding L, Xia R. Organic and solution-processed tandem solar cells with 17.3% efficiency. Science 2018; 361: 1094.
17. Yuan J, Zhang Y, Zhou L, Zhang G, Yip HL, Lau TK, Lu X, Zhu C, Peng H, Johnson PA. Single-Junction Organic Solar Cell with over 15% Efficiency Using Fused-Ring Acceptor with Electron-Deficient Core. Joule 2019; 3: 1140.
18. Wang TL, Shieh YT, Yang CH, Ho TH, Chen CH. Photovoltaic properties and annealing effects of a low bandgapcopolymer containing dithienothiophene and benzothiadiazoleunits. EXPRESS Polym. Lett. 2013; 7(1):63–75.
19. Park MS, and Kim FS. Synergistic Effects of Processing Additives and Thermal Annealing on Nanomorphology and Hole Mobility of Poly(3-hexylthiophene) Thin Films, Polymers. 2019; 11: 112.
20. Bi YG, Liu YF, Zhang XL, Yin D, Wang WQ, Feng J, Sun HB. Ultrathin metal films as the transparent electrode in ITO-free organic optoelectronic Devices. Adv. Opt. Mater. 2019;7: 1800778.
21. Lee HB, Jin WY, Ovhal MM, Kumar N, Kang JW. Flexible transparent conducting electrodes based on metal meshes for organic optoelectronic device applications: A review. J. Mater. Chem. C 2019;7: 1087-1110.
22. Zhang S, Qin Y, Zhu J, Hou J. Over 14% Efficiency in Polymer Solar Cells Enabled by a Chlorinated Polymer Donor. Adv. Mater. 2018; 30: 1800868.
23. Cheng P, Yan C, Lau TK, Mai J, Zhan X. Molecular Lock: A Versatile Key to Enhance Efficiency and Stability of Organic Solar Cells. Adv. Mater. 2016; 28: 5822–5829.
24. Schuller JA, Barnard ES, Cai W, Jun YC, White JS, Brongersma ML. Plasmonics for extreme light concentration and manipulation. Nat. Mater. 2010; 9: 193-204.